EMPIRICAL MODELS FOR PREDICTING LATERAL SPREADING AND EVALUATION USING NEW ZEALAND DATA

Jian Zhang[1], Dick Beetham[2], Grant Dellow[2], John X. Zhao[2] and Graeme H. McVerry[2]

ABSTRACT

A New empirical model has been developed for predicting liquefaction-induced lateral spreading displacement and is a function of response spectral displacements and geotechnical parameters. Different from the earlier model of Zhang and Zhao (2005), the application of which was limited to Japan and California, the new model can potentially be applied anywhere if ground shaking can be estimated (by using local strong-motion attenuation relations). The new model is applied in New Zealand where the response spectral displacement is estimated using New Zealand strong-motion attenuation relations (McVerry *et al.* 2006). The accuracy of the new model is evaluated by comparing predicted lateral displacements with those which have been measured from aerial photos or the width of ground cracks at the Landing Road bridge, the James Street loop, the Whakatane Pony Club and the Edgecumbe road and rail bridges sites after the 1987 Edgecumbe earthquake. Results show that most predicted errors (defined as the ratio of the difference between the measured and predicted lateral displacements to the measured one) from the new model are less than 40%. When compared with earlier models (Youd *et al.* 2002, Zhang and Zhao 2005), the new model provides the lowest mean errors.

1.0 INTRODUCTION

Liquefaction-induced lateral spreading has attracted attention as a potentially damaging seismic hazard. In New Zealand, locations with lateral spreading after the 1987 Egecumbe earthquake have been well documented by Pender and Robertson (1987) and Christensen (1995). Among the locations are the Landing Road bridge, the Thompson Road, the banks of the Whakatane River near the Landing Road bridge, the James Street loop, the Whakatane pony club, and the dairy factory and the road and rail bridges across the Rangitikei River in Edgecumbe. The variation of liquefaction susceptibility in Whakatane was assessed by Beetham *et al.* (2004) who carried out detailed investigations using the Nakamura method and seismic cone penetrometer tests (SCPT). From the collected data, Beetham *et al.* drew a map showing the variation in liquefaction susceptibility within the Whakatane district, which was divided into several regions of negligible, low to moderate, high, and very high liquefaction susceptibility.

Developing appropriate mitigation strategies for liquefaction-induced lateral spreading requires estimating as accurately as possible likely displacements. Two types of models are commonly used to predict liquefaction-induced lateral displacement. One type predicts lateral displacement as a function of earthquake parameters (e.g. magnitude and source distance), soil properties (e.g. mean grain size of granular materials), and topographic data. This model type has been reviewed by Zhang and Zhao (2005). The second model type uses data derived from SPT and/or CPT tests and the relationship between the maximum cyclic shear strain and the factor of safety against liquefaction for different relative densities to predict lateral displacement. This type of model will not be discussed further, because it is based on the acquisition of SPT and/or CPT tests. Readers interested in the second type of model can refer to the paper by Zhang *et al.* (2004) for a detailed introduction.

As an extension to the first type of model, Zhang and Zhao (2005) recently proposed a suite of models for predicting lateral displacement, where predicted lateral displacement, LD, is a function of spectral displacement, SD, as well as soil properties and topographic parameters. However, in estimating the spectral displacement, either the Japanese (Takahashi *et al.* 2003) or the Sadigh *et al.* (1997) strong-motion attenuation relations were applied to all the LD data. In the manner, this approach ignores the fact that a strong-motion attenuation relation is commonly suitable for some regions, rather than anywhere, even if tectonic setting, faulting mechanism, magnitude, and source distance used are identical. We have developed a new empirical lateral displacement prediction model to address this issue. The approach for developing the new model is that we applied an attenuation model developed for Japan to estimate ground motions that may have been associated with Japanese lateral displacement data, and a western US model for western US data, and then used multi-linear regression analysis to derive the new model. By developing the new model in terms of expected ground motions rather than as a function of magnitude and distance, in addition to soil properties and topography of the site, it potentially has universal applicability, provided that ground shaking for a specific site can be directly estimated from local strong-motion attenuation relations. For example, in New Zealand the ground shaking can be estimated using the New Zealand strong-motion attenuation relations of McVerry *et al.* (2006).

The new model is evaluated using the lateral displacements measured in the Landing Road bridge (LRB), the James Street loop (JSL), the Whakatane Pony Club (WPC), and the Edgecumbe road and rail bridges (ERB) after the 1987 Edgecumbe earthquake. The predicted lateral displacements from the new model are compared with those from the Youd *et al.* model (2002) and the Zhang and Zhao models (2005).

[1] *GNS Science, Lower Hutt, New Zealand, Southwest Jiao Tong University, China*
Email: J.Zhang@gns.cri.nz
[2] *GNS Science, Lower Hutt, New Zealand*

2.0 DEVELOPMENT OF EMPIRICAL MODELS FOR PREDICTING LATERAL SPREADING

The lateral spreading displacement dataset of Youd (Youd's website) contains data collected from several countries (mainly Japan and California) and has been used for developing liquefaction-induced lateral spreading prediction models. In the dataset, earthquakes from different tectonic settings (ie. crustal and subduction earthquakes) are mixed together. For example, the 1964 Alaska and the 1983 Nihonkai-Chubu earthquakes are subduction-interface earthquake events while the other earthquakes are crustal events. Similarly, crustal earthquakes with different fault mechanisms are also mixed together (e.g. the 1906 San Francisco earthquake is a strike-slip event, the 1964 Niigata earthquake is a reverse faulting event and the 1983 Borah earthquake is a normal faulting event). If the combined lateral spreading data from earthquakes with different tectonic settings and faulting mechanisms are used as input for the development of empirical models, then a known source of error will be carried forward through the multi-linear regression analysis, because it is known that different fault mechanisms and tectonic settings have a significant impact on ground shaking. For example, the Japanese strong-motion attenuation relations (Zhao *et al.* 2006) predict that the spectral acceleration at 0.5s spectral period for identical earthquake magnitude and source distance to the site from subduction interface earthquake is about 95% of the spectral acceleration from a crustal earthquake event with a strike-slip faulting mechanism and 74% of the spectral acceleration from crustal earthquake with a reverse faulting mechanism.

In order to overcome these drawbacks in the data set, Zhang and Zhao (2005) used strong-motion attenuation relations to estimate ground shaking at locations with lateral spreading data. The estimated ground shaking is used in multi-linear regression to fit the observed lateral displacements. This approach differs from that used by Youd *et al.* (2002), where magnitude and source distance were used in the multi-linear regression. Because most of the measured lateral displacements in Youd's dataset are from Japan and California, Zhang and Zhao (2005) developed two lateral displacement prediction models. One used a Japanese strong-motion attenuation relation (Takahashi *et al.* 2004) and the other used the Sadigh *et al.* attenuation model (1997) for crustal earthquakes and the Youngs *et al.* attenuation model (1997) for subduction zone earthquakes. All data were applied to both models, rather than selecting the relation appropriate to the region producing the data point. Therefore the models of Zhang and Zhao (2005) are only suitable for use in Japan and California or places with similar seismicity to Japan and California.

In the new model, a Japanese attenuation model (Zhao *et al.* 2006) was used to estimate the ground shaking in Japan, and the Sadigh *et al.* (1997) (for crustal earthquakes) and Youngs *et al.* (1997) (for subduction zone earthquakes) models were used to estimate the ground shaking in other parts of the world. Most of the data from outside Japan is from the western US. Therefore, using the Sadigh *et al.* and Youngs *et al.* combination to data from the non-western US has little effect on the new model. The estimated ground shaking is then used in the multi-linear regression analysis. In the procedure, predicted lateral displacements are a function of the strength of ground shaking, soil properties, and topographic parameters. Our hypothesis is that the new model is suitable for the places if a local (or appropriate) strong-motion attenuation model can be used to estimate the ground shaking. For example, the ground shaking estimated from the New Zealand strong-motion attenuation relations (McVerry *et al*., 2006) differs that from the Japanese or the Sadigh *et al.* attenuation models, as shown in Figure 1, even though the comparisons were performed for identical faulting mechanism, tectonic setting and magnitude. However, the approach used in the new model ignores the fact that multiple attenuation relations exist for both Japan and the western US, some of which give quite different estimates especially for near-source areas. In addition, the approach does not take account of the uncertainty in the attenuation models. Both of these points are worthy of investigation in future studies.

In the models of Zhang and Zhao (2005), unbiased estimates against magnitude and source distance (i.e. having zero mean residuals with respect to magnitude and source distance) were obtained at a period of 0.5s for the Japanese and the Sadigh *et al.* attenuation models and at a period of 1.0s for the Youngs *et al.* attenuation model. The inconsistent periods cause difficulties when using the New Zealand strong-motion attenuation relations. This is because for subduction zone earthquakes which period, 0.5s or 1.0s, should be used to estimate the ground shaking? We noted that 1.0s spectral period is only used by the Youngs *et al.* attenuation models for the 1964 Alaska earthquake. The data from the 1964 Alaska earthquake is only 1.45% of the total data set. We are more concerned to have unbiased estimates against magnitude and source distance rather than tolerating the bias, therefore the measured lateral displacements from the 1964 Alaska earthquake were deleted from the dataset.

Investigations of liquefaction-induced lateral spreading caused by strong shaking show that lateral displacements occur in two cases, one near a steep slope, such as adjacent to the edge of a river bank, and the other on gently sloping ground far away from a steep slope (Barlett and Youd, 1995). Normally the lateral displacements from the first case are larger than those from the second one. Hereafter the two cases are called the free-face case and the ground-slope case, respectively, as in Barlett and Youd (1995) and Youd *et al* (2002). We developed separate models for modelling the ground-slope case (Equation 1a) and the free-face case (Equation 1b), but the two models were linked in the regression analysis by using the dummy variable approach, with different indexes to represent different cases, while other terms are common to both models, e.g. the $Log_{10}(SD)$ term in equations 1a and 1b. Note that for some sites, the worse case should be selected by comparing the results from the two cases, because no strict criteria exist for separating the two cases. In Equation 1, ground shaking, in terms of spectral displacement, was derived from strong-motion attenuation relations at 0.5s period and for soil site conditions, generally similar to NEHRP Class D (stiff soil with 180 m/s < V_s < 360 m/s, V_s= the average shear wave velocity in the top 30 m). The selection of this period gave unbiased estimates of lateral displacements with respect to magnitude and source distance, as shown by the residual plots in Figure 2.

For the ground-slope case:

$$Log_{10}(D_h) = 1.8439\ Log_{10}(SD) + 0.4603\, Log_{10}S_{gs} + 0.0197\ T_{15} + 2.4102\ Log_{10}(100 - F_{15}) - 0.8339\ Log_{10}(D50_{15} + 0.1) - 2.6396 \quad (1a)$$

For the free-face case:

$$Log_{10}(D_h) = 1.8439\ Log_{10}(SD) + 0.6096\ Log_{10}W_{ff} + 0.0337\ T_{15} + 2.4102\ Log_{10}(100 - F_{15}) - 0.8339\ Log_{10}(D50_{15} + 0.1) - 3.3689 \quad (1b)$$

where the standard deviation for equation 1 is $\sigma_{Log10(Dh)} = 0.18$. The parameter $D_h = D_{LL}+0.01$ in metres, and other parameters are as follows.

- D_{LL} the lateral-spread displacement
- SD the pseudo-spectral displacement in metres and equal to $SA(0.5s)/(4\pi)^2$
- SA the spectral acceleration in m/s^2, estimated from a strong-motion attenuation model at 0.5s period for sites similar to NEHRP D
- T_{15} the cumulative thickness (in metres) of saturated granular layers with corrected blow counts of $(N_1)_{60}<15$
- S_{gs} the ground slope as a percentage
- W_{ff} the free-face ratio defined as the height (H) of the free face divided by the distance (L) from the base of the free face to the position of the measured displacement, as a percentage
- F_{15} the average fines content (fraction of sediment sample passing a No.200 sieve) for granular materials within the saturated granular layers having a thickness T_{15} in percentage
- $D50_{15}$ the average mean grain size for granular materials within the saturated granular layers in millimetres

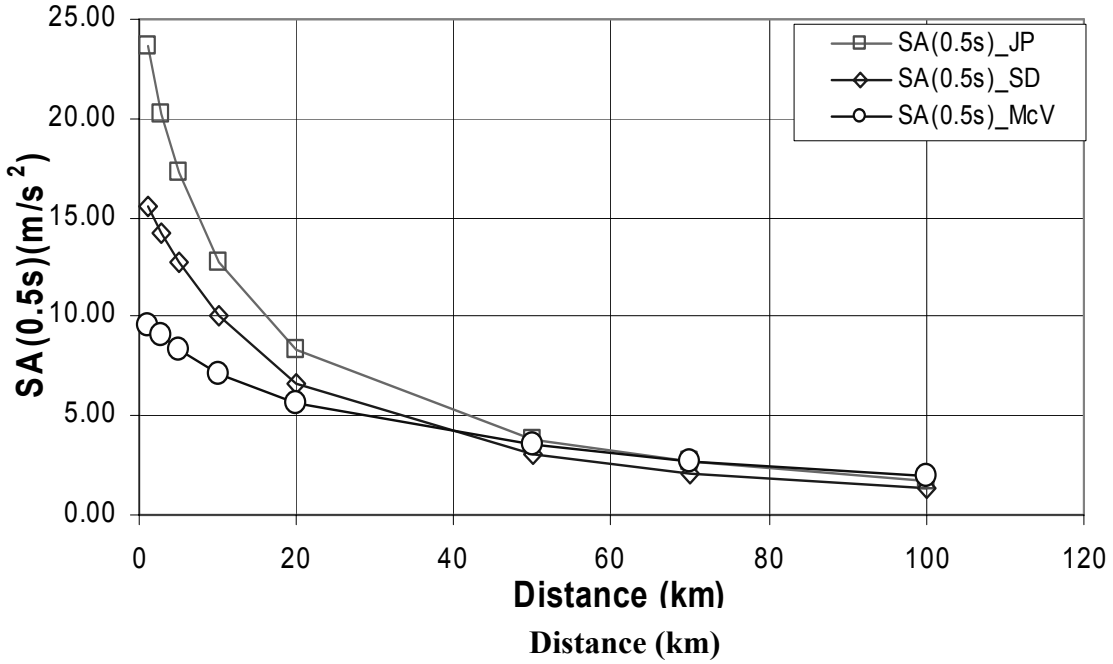

Figure 1. Comparison of estimated spectral accelerations from the Japanese (Zhao et al. 2006), Sadigh et al (1997) and the New Zealand (McVerry et al 2006) strong-motion attenuation models for M_w7.4 strike-slip earthquake with soft soil site conditions for JP, soil site conditions for SD and soft/deep soil site conditions for McV at a period of 0.5s. JP, SD and McV denote the Japanese, Sadigh and the New Zealand attenuation models, respectively. (Note that the Sadigh et al. (1997) model only has two site classes, one class is rock, and the other is soil. Therefore, the soil site class in the Sadigh et al. model is used in the present study).

To assess the sensitivity of the new model, the predicted lateral displacements derived from the new model (Equation 1b) and the models of Zhang and Zhao (2005) for Japan and California are shown in Figure 3. The measured lateral displacements from the 1971 San Fernando earthquake in California and the 1995 Kobe earthquake in Japan are also shown in Figure 3. Parameters T_{15}, W_{ff}, F_{15} and $D50_{15}$ are the averages of the measured values. The spectral accelerations for the 1971 San Fernando earthquake were derived from the Sadigh *et al.* attenuation model (1997) and for the 1995 Kobe earthquake from the Japanese attenuation model (Zhao *et al.* 2006).

For the 1971 San Fernando earthquake (see Figure 3a), the predicted lateral displacements from the new model are close to the mean of the measured values and also close to those from the Sadigh-based Zhang and Zhao expression (2005). The reason for the latter is that the two models were developed based on the measured data from the 1971 San Fernando earthquake.

Figure 3b shows a similar comparison to Figure 3a, but the measured data are from the 1995 Kobe earthquake. In the comparison, the spectral accelerations were estimated by using the Japanese attenuation model (Zhao *et al.* 2006). The comparison shows that the predicted lateral displacements from the new models are slightly higher than those from the model of Zhang and Zhao (2005) for Japan. The predictions from the two models approximate to the mean of the measured lateral displacements.

The results in Figure 3 are expected, because the 1971 San Fernando and the 1995 Kobe earthquakes are larger contributors to Youd's dataset on which both models of Zhang and Zhao (2005) and the new model are based.

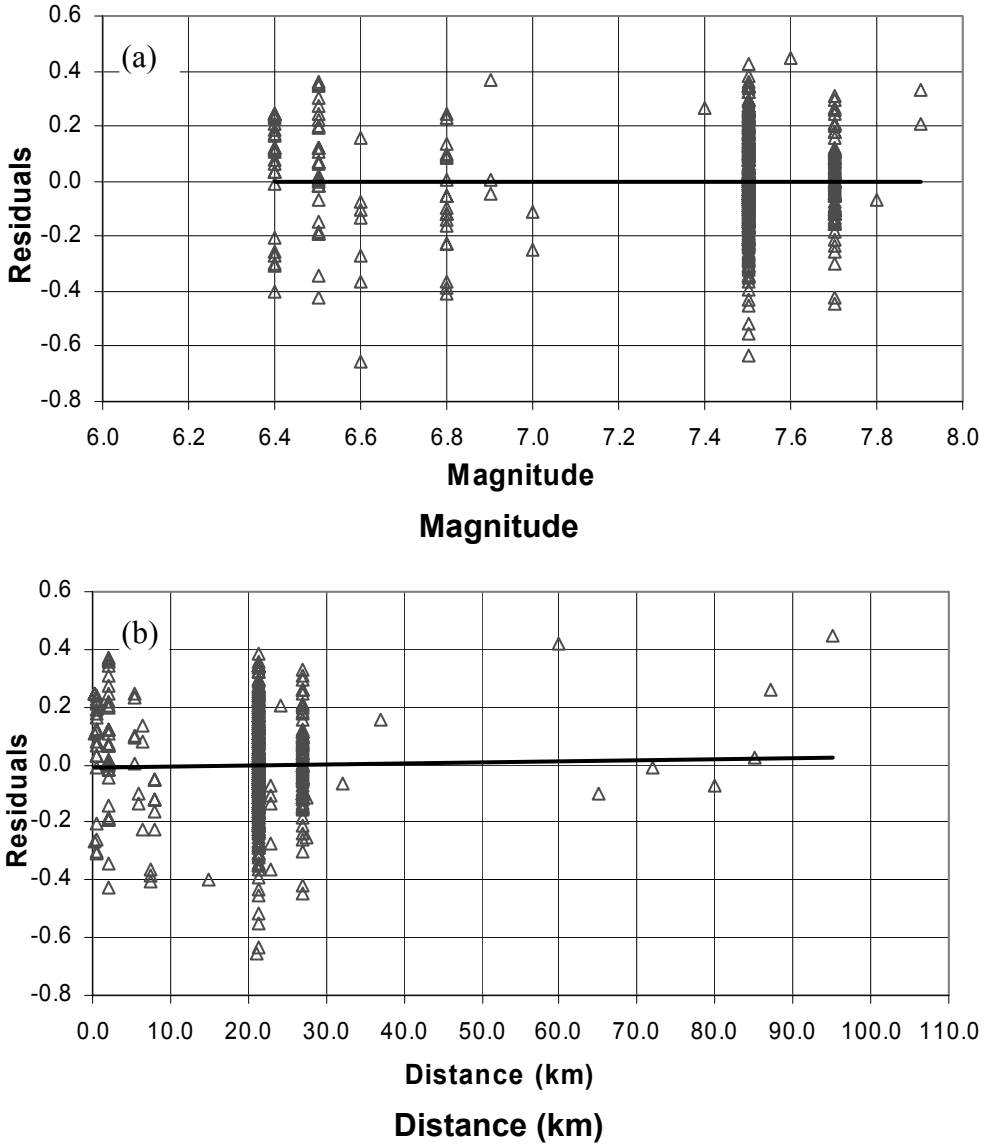

Figure 2. Residuals in log_{10} scale between the predicted (from the new model) and measured lateral displacements from the Youd dataset in log_{10} scale with respect to earthquake magnitude (a) and source distance (b). The solid line is the trend of residuals versus distance.

3.0 Evaluation of the Empirical Model Using Measured Lateral Spreading From the 1987 Edgecumbe Earthquake

The liquefaction-induced damage in the 1987 Edgecumbe earthquake has been well documented. We will use the new model (Equation 1) and the New Zealand strong-motion attenuation relations (McVerry *et al.* 2006) to predict displacement at sites where lateral spreading occurred during the 1987 Edgecumbe earthquake. The predicted lateral displacements will then be to compare with the measured lateral displacements and those predicted by the Youd *et al.* model (2002) and the models of Zhang and Zhao (2005).

The New Zealand strong-motion attenuation relations have been derived from a dataset incorporating all available New Zealand strong-motion data supplemented by a representative selection of overseas near-source strong-motion data. The model is suitable for estimating the ground shaking caused by crustal or subduction zone earthquakes. For crustal earthquakes, the model is suitable for different faulting mechanisms, such as normal-faulting (e.g. the Edgecumbe earthquake).

Lateral spreading displacements from the magnitude M_w6.5 Edgecumbe earthquake were described in Christensen (1995). Among the sites described are the Landing Road bridge (LRB), the James Street loop (JSL), the Whakatane Pony Club (WPC), and the Edgecumbe road and rail bridges (ERB), as shown in Figure 4. At all of these sites infrastructure damage or ground cracking was observed.

At the LRB site, ground cracks attributed to lateral spreading ran parallel to the river bank, except adjacent to the bridge where cracks changed direction relative to the river bank trending at an approximate angle of 45° to both the river bank and the bridge. As a result, the base of the north-western abutment of the bridge rotated about 0.5° towards the river (Christensen 1995). At the JSL and WPC sites, only ground cracking was observed.

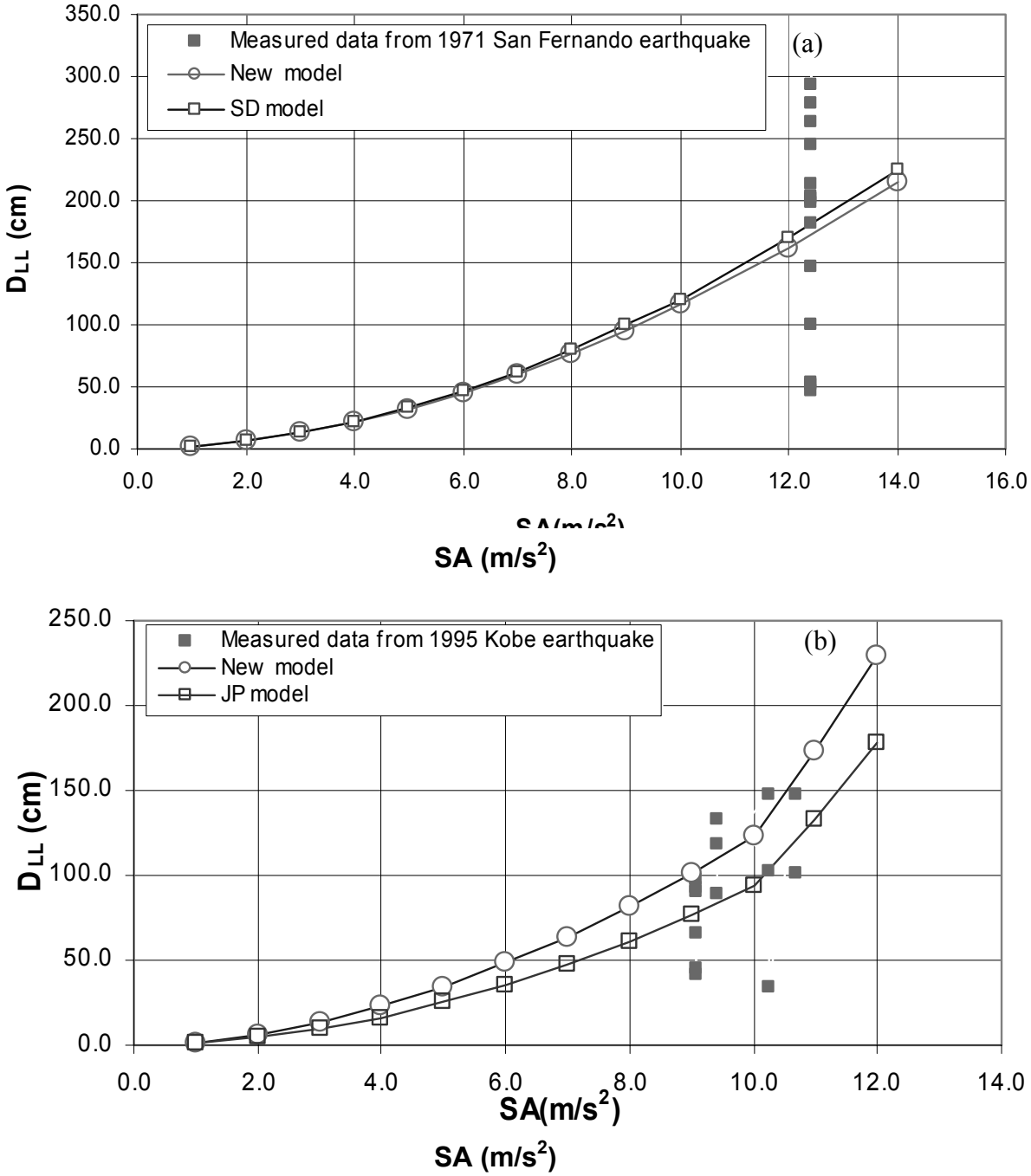

Figure 3. Comparison of the predicted lateral displacements from the new model and the Zhang and Zhao models (2005) using the Sadigh and the Japanese attenuation model and the measured lateral displacements from (a) the 1971 San Fernando earthquake and (b) the 1995 Kobe earthquake. SD and JP models denote the Zhang and Zhao models suitable for California and Japan areas respectively. For the new model, the Sadigh et al. (1997) attenuation model is used for the San Fernando data and the Zhao et al. (2006) model for the Kobe data. Note that the two earthquakes contribute much data to Youd's dataset from which all these models were developed.

To evaluate the accuracy of the new model (Equation 1), the predicted lateral displacements from the model are compared with the measured lateral displacements or the estimated width of ground cracking. At sites with extensive cracking, an assumption is made that a total lateral displacement is the cumulative value of all crack widths from the first crack close to river. The soil properties and topographic parameters required in the new model for these sites were obtained from CPT data in Christensen (1995) or from the report of Pender and Robertson (1987). Some F_{15} were obtained from the work of Bienvenu (1988) and Pender and Robertson (1987).

Lateral displacements at sites LRB, JSL, WPC and ERB were measured and mapped by Christensen. The measured lateral displacements are near, but not at the exact location of CPT sites. In order to use the geotechnical parameters derived from the CPT data, we have used a vector interpolation method, similar to that of Bardet *et al.* (1999). Equation 2 expresses the vector interpolation method. In Equation 2a, $X_{x/y}$ represents

the lateral displacement component in the x or y direction, X_i represents the measured lateral displacement component in the x or y direction at point i, and d_i is the distance from point i to a CPT site. Using this methodology, the lateral displacement component at the CPT site can be determined in the x or y direction. The total lateral displacement at point i is derived by Equation 2b.

$$X_{x/y} = \frac{\sum_{i=1}^{n} X_i / d_i}{\sum_{i=1}^{n} 1/d_i} \quad (2a)$$

$$X = \sqrt{X_x^2 + X_y^2} \quad (2b)$$

In Sections 3.1 to 3.4, comparisons between the predicted and measured displacement values are made for each of the four sites.

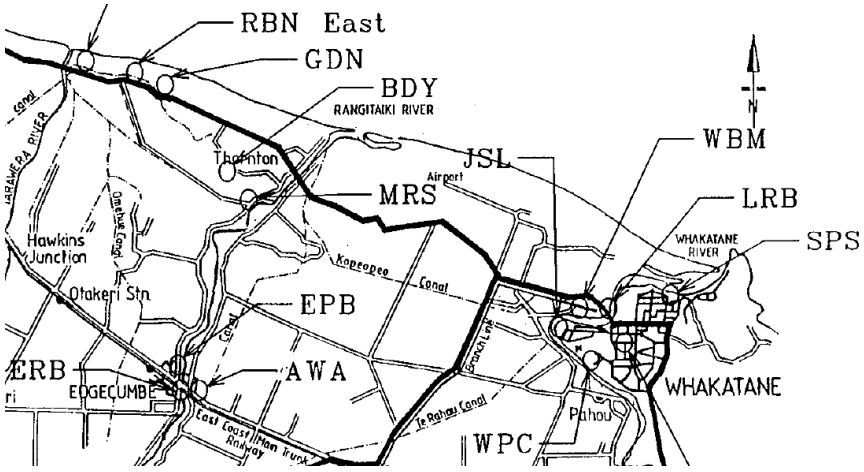

Figure 4. Relative locations of LRB, JSL, WPC, and ERB sites with respect to Whakatane town. The shortest distance to the rupture plane of the 1987 Edgecumbe earthquake is 1.4 km for ERB site and 11 km for others.

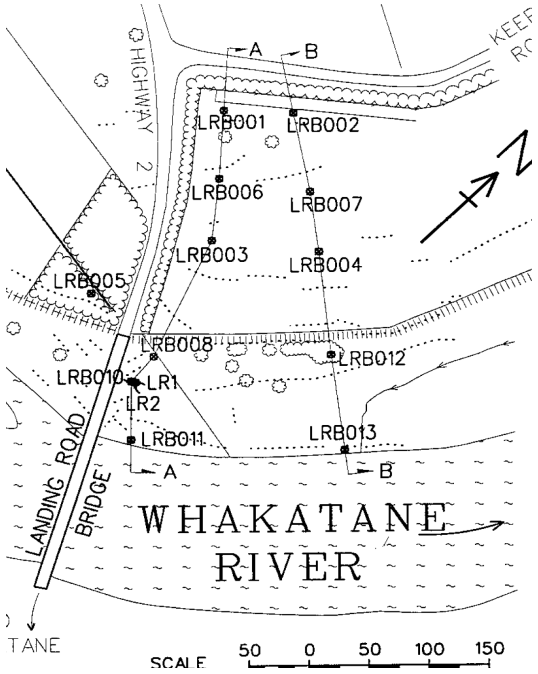

Figure 5. Locations of CPT/SPT stations from LRB001 to LRB013 and ground cracking at Landing Road Bridge site. AA and BB show two sections, black dot denotes CPT/SPT station, and dotted line represents ground crack's location and length. The scale is in metres. (From Figure 8.17 of Christensen).

3.1 Landing Road Bridge Site (LRB)

Christensen (1995) attempted to measure lateral displacements using photogrammetry around the LRB site, but results were erratic and inconclusive. Christensen did, however, observe ground cracks and provided the following description: "In total, beside the bridge, there were about five major crack sequences with a width in excess of 200 mm each in a strip 300 m long beside the true left bank of the river". These cracks are shown in Figure 5, with the first one between stations LRB001 and LRB006, the second between stations LRB003 and LRB005, the third along the stopbank, the fourth between stations LRB008 and LRB011 and passing through station LRB010 and the last one near to the edge of the bank of the river. If each crack had a width of 200 mm, the total lateral displacement would have been about 1 m.

Predicted lateral displacement at the CPT sites from the new model (Equation 1) is plotted against distance to the edge of the river in Figure 6. The maximum predicted lateral displacement is in the range of 400 to 500 mm, approximately half of the estimated total lateral displacement (1 m). In Figure 6, the predicted lateral displacements suddenly increase from LRB003 to LRB008 and from LRB012 to LRB013. This is because along section AA the ground slope at LRB008 is steeper than that at LRB003. Along section BB station LRB013 is closest to the river channel (free-face). Note that apart from stations LRB008, LRB010, LRB011 and LRB013, the predicted lateral displacements at other stations are small. This is because these stations lie in an area that is essentially flat.

A ground crack with 150-300 mm width was mapped 15m northwest of station LRB007. The predicted lateral displacement at station LRB007 is 123 mm from the new model, and 131 mm from the Youd *et al.* model and 202 mm and 335 mm from the models of Zhang and Zhao for Japan and California models respectively. These results show that the differences between the predicted lateral displacements (from the empirical models) and the median crack width are not large. Our predictions are for a mean cumulative lateral displacement, rather than the width of a crack. We noted from Figure 5 that the cumulative displacement at station LRB007 is the sum of the width of two cracks, one at station LRB002 and the other between stations LRB002 and LRB007. The width of the crack at LRB002 is probably small, as it is very short in length (see Figure 5). The width of the crack northwest of station LRB007 is therefore approximately equal to the cumulative displacement at station LRB007.

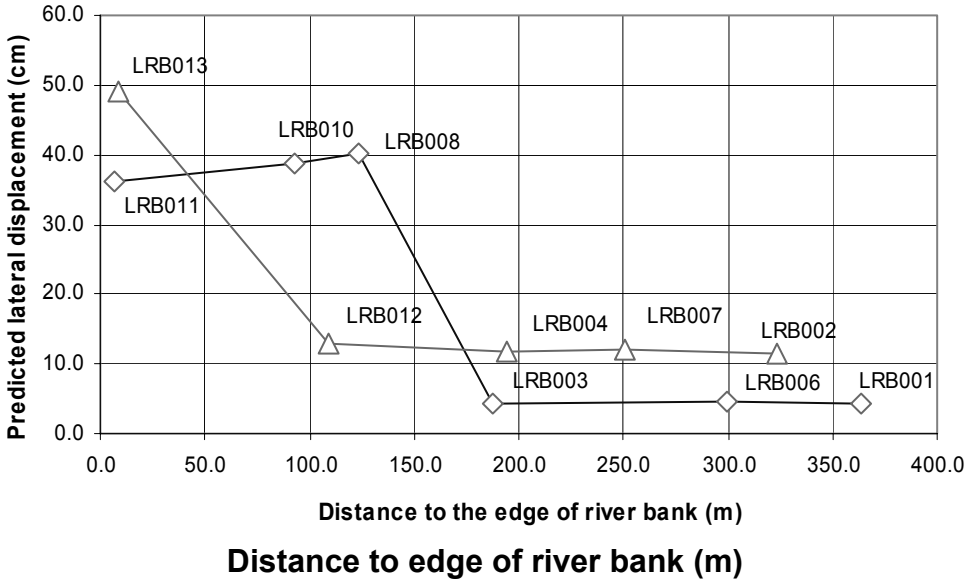

Distance to edge of river bank (m)

Figure 6. Predicted lateral displacement from the new model using the New Zealand attenuation model versus distance to the edge of the river bank along AA and BB sections at Landing Road Bridge site. CTP/SPT stations are also labelled in the figure.

3.2 James Street Loop (JSL)

Figure 7 shows locations of both ground cracking and CPT sites from stations JSL001 to JSL008. Most of the cracks are adjacent to the edge of the river bank. The predicted lateral displacement from the new model at the CPT sites versus distance to the edge of the river is shown in Figure 8. Figure 8 shows that the predicted lateral displacements at JSL004 and JSL005 are 860 mm and 820 mm, respectively, and much larger than those at other stations. This result is expected because stations JSL004 and JSL005 are near the river channel and classified as free-face case, as shown in Table 1.

The lack of measured lateral displacements at the site makes it difficult to ascertain the accuracy of the predicted lateral displacements from Equation 1. Using the empirical lateral displacement prediction model of Hamada (1986), Christensen (1995) predicted a lateral displacement of 1.40 m near to station JSL005. Compared with 1.40 m predicted by Hamada model, the predicted displacement of 820 mm from the new model at station JSL005 (adjacent to the river edge) is low. However, we have noted that the Hamada model was developed based on the measured data from one earthquake event, whereas the new model was developed from a data set derived from many earthquake events.

3.3 Whakatane Pony Club (WPC)

Unlike the Landing Road Bridge and James Street Loop sites, the Whakatane Pony Club site is not close to the Whakatane

River, as shown in Figure 9. Most ground cracks caused by the 1987 Edgecumbe earthquake are parallel to the Awatapu Lagoon. Predicted lateral displacements from the new model at four CPT sites (WPC001 to WPC004) are listed in Table 2.

Christensen (1995) used photogrammetry to measure lateral displacements around the WPC site. We again use the vector interpolation methodology to obtain the lateral displacements at CPT sites. The measured lateral displacements at CPT sites are listed in Table 2, together with the predicted lateral displacements from the Youd *et al.* model (2002) and the models of Zhang and Zhao (2005) for Japan and California. The accuracy of the empirical prediction models is evaluated using an error term, defined as a percentage of the ratio of the difference between the predicted and measured lateral displacements to the measured lateral displacement. The results show that the new model provides the lowest mean error, typically only 40-50 percent of the error of the other models. The predicted lateral displacements from the new model at stations WPC001 and WPC003 are 470 mm and 460 mm, respectively. The predicted lateral displacements from the other models can be found in Table 2. Results show that the models of Zhang and Zhao overestimate lateral spreading, whereas the Youd *et al.* model underestimates it.

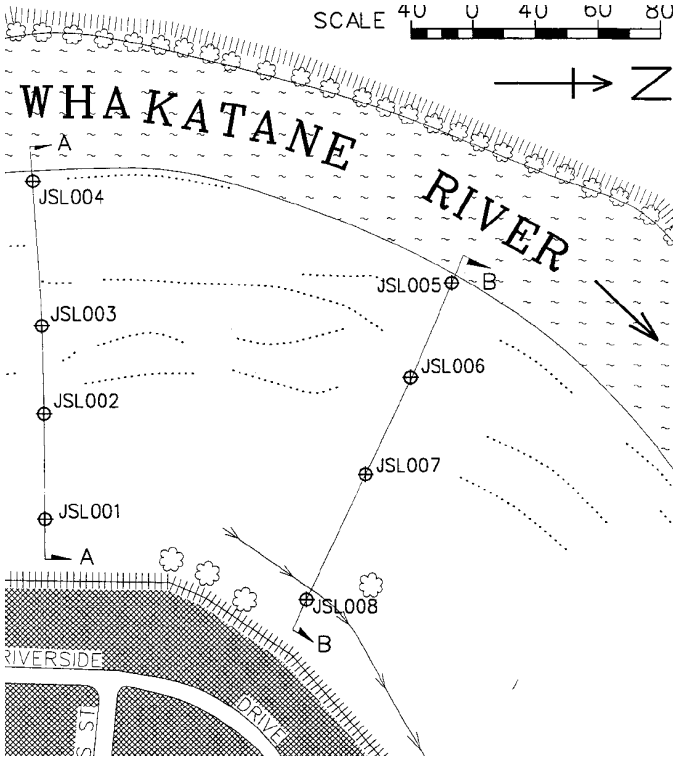

Figure 7. Locations of CPT/SPT stations from JSL001 to JSL008 and ground cracking at James Street Loop site. AA and BB show two sections, circle denotes CPT/SPT station and dotted line represents ground crack. The scale is in metres. (From Figure 8.19 of Christensen).

3.4 Edgecumbe Road and Rail Bridges (ERB)

Near the Edgecumbe Road and Rail Bridges, lateral displacements triggered by the 1987 Edgecumbe earthquake were considered a major cause of damage to the piers of the bridges. Christensen (1995) provided a measured lateral displacement map around the site. As expected, many lateral displacements adjacent to the edge of the Rangitaiki river point to the river channel, indicating that the soils moved forwards to the river.

The lateral displacements at stations ERB001 to ERB005 (shown in Figure 10) are obtained using the vector interpolation method, similar to the WPC site. The predicted and measured lateral displacements are listed in Table 3. In Table 3, mean errors for each of the models are listed to show the accuracy of the prediction from the models. The new model provides the lowest mean error of 40%, and the Youd *et al.* model and the model of Zhang and Zhao for Japan and California have similar mean errors of 400%. For the new model the maximum difference between predicted and measured values is less than 30%, except for station ERB003, which has a difference of 175%. The reason for such a large difference at station ERB003 is that measured displacements around station ERB003 are rare, so displacement vectors at distances of more than 100 m were used in the vector interpolation. Consequently, the measured lateral displacement at station ERB003 may be greatly underestimated.

4.0 DISCUSSION

The comparisons between the measured and predicted lateral displacements at the LRB, JSL, WPC, and EBR sites show that the predicted displacements from the new model (Equation 1) are reasonably consistent with the measured values (most of the differences are 40% or less). Larger differences between the predicted and interpolated lateral displacements were found adjacent to the edge of the river bank at the LBR and ERB sites. Possible reasons are that the interpolated lateral displacements were underestimated at these stations, such as at station ERB003. Similar problems

are also demonstrated in the other empirical models, as shown in Table 3.

Compared with the Youd *et al.* model (2002) and the models of Zhang and Zhao (2005), the new model provides the lowest mean errors for the WPC and EBR sites. Mean errors show that the prediction accuracy from all empirical models for the WPC site (ground-slope case) is higher than for the EBR site (free-face case). The result indicates that a prediction error for free-face case is larger than that for ground slope case. This result is expected because Youd's dataset shows that the maximum measured lateral displacement is 5.4 m for the ground-slope case and 10.2 m for the free-face case, implying a larger scatter in the free-face case than that in the ground-slope case. The empirical models were developed from the Youd dataset, so the prediction error for the free-face case should be larger than that for the ground-slope case, as has been shown in Tables 2 and 3.

In the present study, all the predicted lateral displacements are median values. If ranges of plus and minus two standard deviations are considered, the minimum estimated lateral displacement at station ERB003 is 820 mm, slightly larger than the measured value (720 mm). The maximum estimated lateral displacement at LRB site is 1.17 m, encompassing the sum of widths of all the cracks (1 m). This result illustrates that the predicted error for most data falls in the range of plus or minus one standard deviation, and even the worst errors are only about two standard deviations.

For cases where no measured displacement exists, an alternative approach is to compare predicted lateral displacements with the observed width of ground cracking. Three comparisons have been made. All results show that the observed width of ground cracking is in a good agreement with the predicted ones from the new model.

Table 1. Geotechnical and Topographic parameters for LRB and JSL stations

Station Name		T_{15}	S_{gs}	W_{ff}	F_{15}	$D50_{15}$
Landing Road Bridge Site	LRB001	3.8	0.01		10.1	0.278
	LRB002	3.6	0.09		10.1	0.278
	LRB003	3.95	0.01		10.1	0.278
	LRB004	4.2	0.09		10.1	0.278
	LRB005	4.5	0.71		10.1	0.278
	LRB006	5.2	0.01		10.1	0.278
	LRB007	4.55	0.09		10.1	0.278
	LRB008	4.25	1.32		10.1	0.278
	LRB010	3.5	1.32		10.1	0.278
	LRB011	2.9		15.4	10.1	0.278
	LRB012	5.9	0.09		10.1	0.278
	LRB013	2.4		27.1	10.1	0.278
James Street	JSL001	4.5	0.72		10.0	0.23
	JSL002	4.45	0.72		10.0	0.23
	JSL003	5.35	0.72		10.0	0.23
	JSL004	5.15		33.6	10.0	0.23
	JSL005	4.75		32.7	10.0	0.23
	JSL006	5.70	0.48		10.0	0.23
	JSL007	3.85	0.48		10.0	0.23
	JSL008	3.20	0.48		10.0	0.23

Table 2. Predicted and measured lateral displacements (cm) at the Whakatane Pony Club

Soil properties/ Empirical model	Stations				Mean error[1] (%)
	WPC001	WPC002	WPC003	WPC004	
Observed	57	58	58	57	
Youd Model	30	27	25	24	54
California[2]	85	80	77	76	38
Japan[2]	88	86	84	84	48
New Model	47	46	46	46	20
T_{15}	2.5	2.1	1.8	1.7	
S_{gs}(%)	1.5	1.5	1.5	1.5	
F_{15}(%)	10	10	10	10	
$D50_{15}$	0.204	0.204	0.204	0.204	

1 Error (%) = 100* |(Measured-Predicted)/Measured|

2 California and Japan denote the Zhang and Zhao model suitable for California and Japan areas

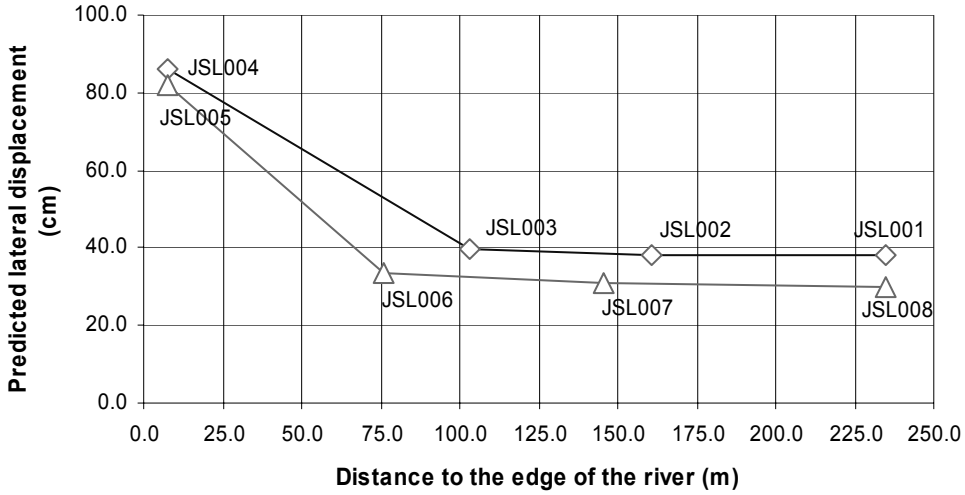

Figure 8. Predicted lateral displacement from the new model using the New Zealand attenuation model versus distance to the edge of the river bank at James Street Loop along sections A-A and B-B. The names of CPT/SPT stations are also labelled in the figure.

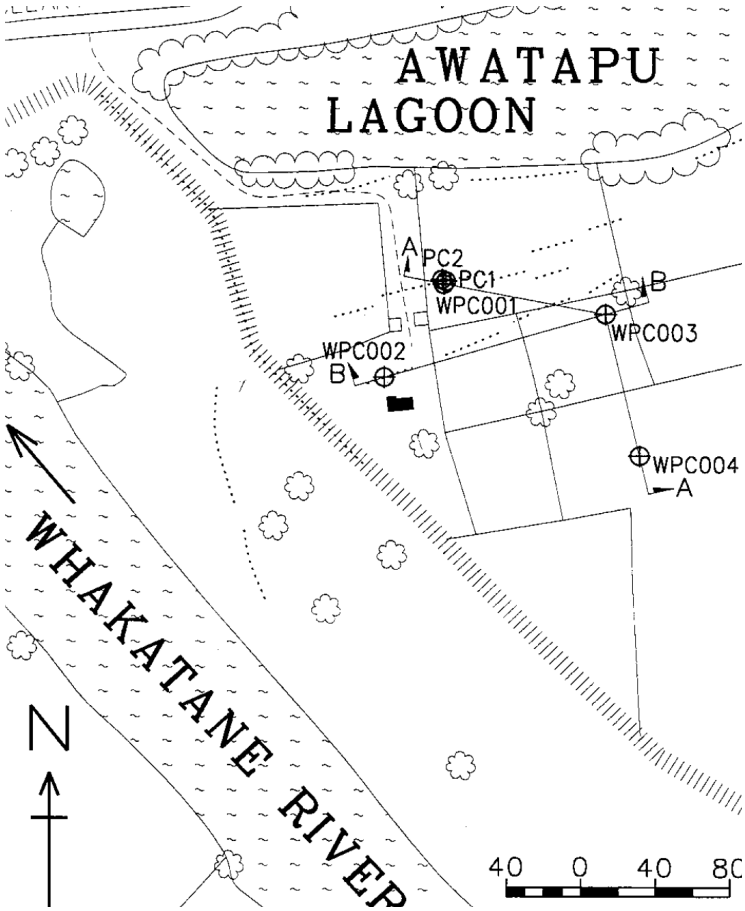

Figure 9. Locations of CPT/SPT stations from WPC001 to WPC004 and ground cracking at Whakatane Pony Club site. Circle denotes CPT/SPT station and dotted line represents ground crack. The scale is in metres. (From Figure 8.26 of Christensen).

Table 3. Predicted and measured lateral displacements (cm) at the Edgecumbe Rail Bridge

Soil Properties/ Empirical model	Stations					Mean error[1] (%)
	ERB001	ERB002	ERB003	ERB004	ERB005	
Observed	69	70	72	94	68	
Youd Model	196	348	841	338	196	419
California[2]	221	320	644	340	221	371
Japan[2]	227	335	744	387	227	417
New Model	61	88	199	110	61	39
T_{15}	1.7	3.1	4.4	1.6	1.7	
W_{ff}(%)	6.3	9.6	31.0	16.7	6.3	
F_{15}(%)	23	23	23	23	23	
$D50_{15}$	0.062	0.062	0.062	0.062	0.062	

[1] Error(%)=100* | (Measured-Predicted)/Measured |

[2] California and Japan denote the Zhang and Zhao model suitable for California and Japan areas

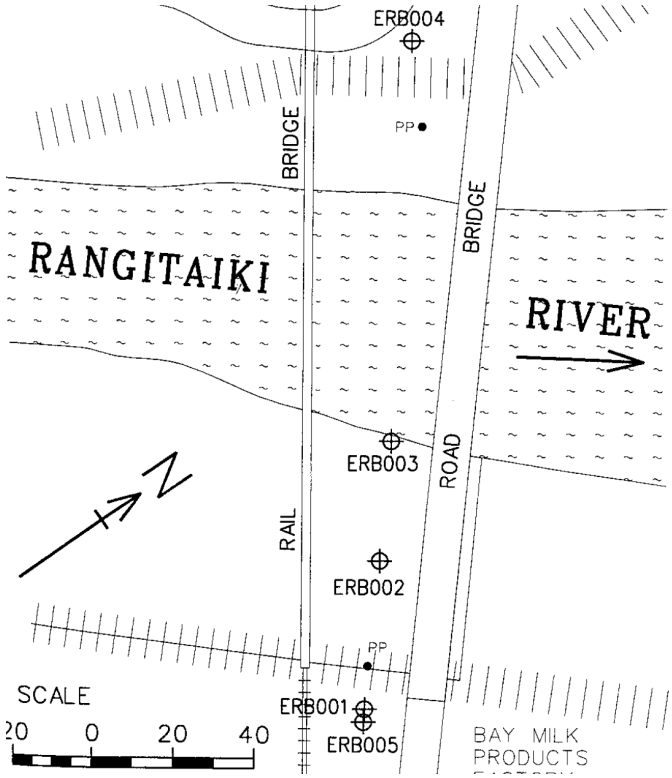

Figure 10. Locations of CPT/SPT stations from ERB001 to ERB005 at Edgecumbe Road and Rail Bridges site. Circle represents CPT/SPT station. (From Figure 8.35 of Christensen).

5.0 CONCLUSIONS

Based on the above analyses, the following conclusions are reached:

1. An new empirical model for predicting liquefaction-induced lateral spreading displacement as a function of 5% damped spectral displacements has been developed and applied in New Zealand. The new model extends the application of Zhang and Zhao's model (2005), which is suitable for use in Japan and California and areas where attenuation relations developed for Japan and/or the western US are applicable;
2. Predicted lateral spreading displacements from the new model are comparable with the results from the Zhang and Zhao models (2005) for earthquake events with strike-slip and reverse-faulting mechanisms. These two earthquake mechanisms provide much of the data in the Youd's dataset that was used in the development of both models. Differences exist, but are not large, indicating that the new model is reasonably consistent with previous work.
3. To evaluate the new model, measured lateral spread displacements at sites LRB, JLS, WPC and ERB in the 1987 Edgecumbe earthquake were compared with the predictions from the new model. In the procedure, the

New Zealand strong-motion attenuation relations were used to estimate the ground shaking. The results show that differences between the predicted and measured lateral displacements for the new model are less than 40% (typically 20 - 40%). Thus the predicted lateral displacements from the new model are in a reasonable agreement with the measured lateral displacements;

4. Further comparisons have been carried out with the predicted lateral spreading displacements from the Youd *et al.* model (2002) and the Zhang and Zhao models (2005) for LRB, JLS, WPC and ERB sites. The results show that for most cases the new model provides the lowest mean errors among all the empirical models in the present study.

5. The accuracy of the new model for those stations adjacent to the edge of river banks is less satisfactory. For station ERB003, the poor accuracy probably is from underestimating the actual lateral displacement. Even then, the worst prediction errors are within ± 2 standard deviations of the median predictions of equation 1.

6.0 ACKNOWLEDGEMENTS

The authors wish to thank Chris Massey for his helpful in-house review. This study is supported in part by the Foundation for Research and Science and Technology of New Zealand, Contract number C05X0402.

7.0 REFERENCES

Bardet, J-P., Mace, N. and Tobita, T. (1999). "Liquefaction-induced Ground Deformation and Failure", *Department of Civil Engineering, University of Southern California*, A report to PEER/PG&E, Task 4A - Phase

Bartlett, S.F. and Youd, T.L. (1995). "Empirical prediction of lateral spread displacement." *J. Geotech Engng*; **121**(4): 316-329.

Beetham, R., Dellow, G., Cousins, J., Mouslopoulou, V., Hoverd, J., Gerstenberger, M., Stephenson, B., Davenport, P. and Barker, P. (2004). "Whakatane Microzoning Study", *Institute of Geological & Nuclear Sciences, Client Report 2004/18.*

Bienvenu, V. (1988). "Studies of liquefaction in 1929 Murchison and 1968 Inangahua, New Zealand earthquakes", Master of Engineering Thesis, *University of Canterbury,* Christchurch, New Zealand.

Christensen, S.A. (1995). "Liquefaction of Cohesionless Soils in the March 2, 1987 Edgecumbe Earthquake, Bay of Plenty, New Zealand, and Other Earthquakes", *University of Canterbury*, Department of Civil Engineering, January.

Cousins, W.J., Zhao, J.X. and Perrin, N.D. (1999). "A model for the attenuation of peak ground acceleration in New Zealand earthquakes based on seismograph and accelerograph data." *Bulletin of the NZ Society for Earthquake Engineering*; **32**(4): 193-217.

Hamada, M., Yasuda, S., Isoyama, R. and Emoto, K.(1986). "Study on liquefaction-induced permanent ground displacement". Report for the Association for the Development of Earthquake Prediction.

McVerry, G.H., Zhao, J.X., Abrahamson, N.A. and Somerville, G.H. (2006). "New Zealand acceleration response spectrum attenuation relations for Crustal and Subduction earthquakes", *Bulletin of the New Zealand Society for Earthquake Engineering*, **39**(1): 1-58.

Pender, M.J. and Robertson, T.W. (1987). "Edgecumbe Earthquake: Reconnaissance Report." *Bulletin of the NZ Society for Earthquake Engineering*; **20**(3): 201-248.

Sadigh, K., Chang, C.-Y., Egan, J.A., Makdisi, F. and Youngs, R.R. (1997). "Attenuation relationships for shallow crustal earthquakes based on California strong motion data", *Seismological Research Letters*; **68**(1): 180-189.

Youd, T.L., website: www.et.byu.edu/ce/ceen.php?page=youd/liq.htm

Youd, T.L., Hansen, C.M. and Bartlett, S.F. (2002). "Revised multilinear regression equations for prediction of lateral spread displacement." *J. Geotech and Geoenvironmental Engng*; **128**(12): 1007-1017.

Youngs, R.R., Chiou, S-J., Silva, W.J. and Humphrey, J.R. (1997). "Strong ground motion attenuation relationships for subduction zone earthquakes." *Seismological Research Letters*; **68**(1): 58-73.

Takahashi, T., Saiki, T., Okada, H., Irikura, K., Zhao, J.X., Zhang, J., Thio, H.K., Somerville. P.G., Fukushima, Y. and Fukushima, Y. (2004). "Attenuation models for response spectra derived from Japanese strong-motion records accounting for tectonic source types." *13th WCEE*, Canada, Paper No.1271.

Zhang, G., Robertson, P.K. and Brachman, R.W.I. (2004). "Estimating Liquefaction-Induced Lateral Displacements Using the Standard Penetration Test or Core Penetration Test." *J. Geotech and Geoenvironmental Engng*; **130**(8): 861-871.

Zhang, J. and Zhao, J.X. (2005). "Empirical Models for Estimating Liquefaction-Induced Lateral Spread Displacement", *Soil Dynamics and Earthquake Engineering*; **25**: 439-450.

Zhao, J.X., Zhang, J., Asano, A., Ohno,Y., Oouchi, T., Takahashi, T., Ogawa, H., Irikura, K., Thio, H.K., Somerville, P.G., Fukushima, Y. and Fukushima Y. (2006). "Attenuation relations of strong ground motion in Japan using site classification based on predominant period", *Bulletin of the Seismological Society of America*, in press.

APPENDIX

The New Zealand strong-motion attenuation models (McVerry *et al.* 2006) have been used in the new lateral displacement prediction models.

For crustal earthquakes SA_{CRU}(0.5s) :

$$LnSA^*_{CRU}(0.5s) = 1.3826 - 0.144\,M_w - 0.0635(8.5 - M_W)^2 - 0.00823\,R + (-1.58716 + 0.17M_W)Ln(R^2 + 18.49)^{0.5} - 0.0326\,R_{VOL} + 0.2\,CN + 0.119\,CR + -0.121\,Ln(PGA^*_{rock} + 0.03) \quad \text{(A1)}$$

$$LnPGA^*_{rock} = 1.0453 - 0.144M_W - 0.00846R + (-1.77519 + 0.17M_W)\,Ln(R^2 + 31.36)^{0.5} - 0.03301R_{VOL} + 0.2CN + 0.26CR \quad \text{(A2)}$$

$$LnSA^*_{CRU}(0) = LnPGA^*_{rock} - 0.23Ln(PGA^*_{rock} + 0.03) - 0.29648 \quad \text{(A3)}$$

$$LnPGA_{rock} = 1.15215 - 0.144M_W - 0.00967\,R + (-1.72494 + 0.17M_W)\,Ln(R^2 + 31.36)^{0.5} - 0.03279\,R_{VOL} + 0.2\,CN + 0.26\,CR \quad \text{(A4)}$$

$$LnSA_{CRU}(0) = LnPGA_{rock} - 0.23Ln(PGA_{rock} + 0.03)) - 0.31769 \quad \text{(A5)}$$

$$SA_{CRU}(0.5s) = SA^*_{CRU}(0.5s) * (SA_{CRU}(0) / SA^*_{CRU}(0))$$

For subduction zone earthquakes SA_{SUB}(0.5s):

$$LnSA^*_{SUB}(0.5s) = 0.19699 + 1.43965M_W - 0.0048(10 - M_W)^3 - 2.4063Ln(R + 1.7818\exp(0.554M_W)) + 0.01287H_C - 0.24839SI - 0.0326R_{VOL}(1 - DS) - 0.121Ln(PGA^*_{rock} + 0.03) \quad \text{(B1)}$$

$$LnPGA^*_{rock} = -0.16415 + 1.37852M_W - 2.48795Ln(R + 1.7818 * e^{0.554M_W}) + 0.01622H_C - 0.41369 * SI - 0.03301R_{VOL}(1 - DS) \quad \text{(B2)}$$

$$LnSA^*_{SUB}(0) = LnPGA^*_{rock} - 0.23Ln(PGA^*_{rock} + 0.03) - 0.29648 \quad \text{(B3)}$$

$$LnPGA_{rock} = 0.14878 + 1.42246M_W - 2.56727Ln(R + 1.7818\exp(0.554M_w)) + 0.0155H_c - 0.50962SI - 0.03279R_{VOL}(1 - DS) \quad \text{(B4)}$$

$$LnSA_{SUB}(0) = LnPGA_{rock} - 0.23Ln(PGA_{rock} + 0.03)\text{ -0.31769} \quad \text{(B5)}$$

$$SA_{SUB}(0.5s) = SA^*_{SUB}(0.5s) * (SA_{SUB}(0) / SA^*_{SUB}(0)) \quad \text{(B6)}$$

where M_w is moment magnitude; R is shortest distance to the rupture plane in km; CN is -1 for normal fault and 0 otherwise; CR is 0.5 for reverse/oblique fault, 1 for reverse fault and 0 otherwise; SI is 1 for interface earthquakes and 0 otherwise; DS is 1 for deep slab earthquakes and 0 otherwise; H_c is the centroid depth in km, R_{vol} is length in km of the part of the source-to-site path in the volcanic zone.

The final values of spectral accelerations are $SA_{CRU}(0.5s)$ and $SA_{SUB}(0.5s)$ at a period of 0.5s, derived from Eqs.A6 and B6. $SA^*_{CRU}(0.5s)$ and $SA^*_{CRU}(0.5s)$ are initial values derived directly from the response spectrum dataset. It was found that this

dataset gave smaller values than many other well-known response spectrum models. It was also found in modelling peak ground accelerations that using a larger dataset incorporating some records that had only peak ground accelerations without spectra gave stronger PGAs than those modelled from the response spectrum dataset. The stronger PGAs from the overall dataset were more in line with other models. For this reason, we have multiplied the initial spectral values (e.g. $SA^{*}_{CRU}\left(0.5s\right)$) by the PGA ratio (e.g. $SA_{CRU}\left(0\right)/SA^{*}_{CRU}\left(0\right)$) to obtain the final spectral values (e.g. $SA_{CRU}\left(0.5s\right)$).